High Resolution Electronic Spectrum of the N_2 van der Waals Complex of *p*-Difluorobenzene. Structure and Internal Motion†

Martin Schäfer

Laboratorium für Physikalische Chemie, Eidgenössische Technische Hochschule Zürich, CH-8093 Zürich, Switzerland

Cheolhwa Kang and David W. Pratt*

Department of Chemistry, University of Pittsburgh, Pittsburgh, Pennsylvania 15260

Received: May 3, 2003; In Final Form: August 12, 2003

Rotationally resolved fluorescence excitation spectra of the N_2 van der Waals complex of *p*-difluorobenzene (*p*DFB−N_2) have been recorded in the collision-free environment of a molecular beam. The data obtained provide information about the structure and internal motion of *p*DFB−N_2 in its ground (S_0) and excited (S_1) electronic states. In the ground state, the N_2 molecule sits at $R \sim 3.5$ Å above the ring plane, is parallel to the short axis of the ring, and undergoes hindered internal rotation about the axis perpendicular to the ring with an apparent 2-fold barrier of $\sim$10 cm^{-1}. Excitation to the S_1 state decreases R by $\sim$0.1 Å and reduces the barrier to $\sim$2 cm^{-1}. The N_2 molecule appears to have no preferred orientation in the S_1 state. Photoinduced changes in the π-electron distribution are responsible for this behavior. Despite this fact, the S_1-S_0 transition moment orientation in *p*DFB is unaffected by complex formation.

Introduction

Weakly bound van der Waals (vdW) complexes between aromatic molecules and rare gases or small molecules have been the focus of much recent attention, for many reasons. One reason is that such complexes are unique chemical species, with their large vdW bond distances of 3−5 Å, their low bond energies of only a few hundred wavenumbers, and their large amplitude, low-frequency vibrational motions. Another reason is that the properties of such species reveal information about solvent−solute interactions in cases where dispersion forces are dominant. And another reason is that the dynamic process of vibrational predissociation (VP) of vdW complexes also provides a testing ground for theories of collision dynamics, intramolecular vibrational redistribution (IVR), and dissociation dynamics. All are fundamental to chemical reactivity.

We focus in this report on one such species, the vdW complex of N_2 and *p*-difluorobenzene (*p*DFB−N_2). Our attention was drawn to this complex when it was reported, on the basis of a study of the rotational contour of the 6_0^1 band in its S_1-S_0 electronic spectrum, that the electronic transition moment (TM) was rotated by about 30° toward the F−F axis, from its position normal to that axis in the bare molecule.[1] Conformationally induced changes in the orientation of an electronic TM have been observed, especially in substituted benzenes.[2] But such a large, *complex*-induced change in the orientation of an electronic TM would be unprecedented.

Molecular nitrogen complexes of several aromatic molecules have been studied before, including benzene−N_2,[3−6] *p*DFB−N_2,[7−9] *m*DFB−N_2,[9] *o*DFB−N_2,[9] $C_6H_5X-N_2$ (X = F, Cl, Br),[10] phenol−N_2,[11] aniline−N_2,[12,13] benzyl−N_2,[14] and cyclopentadienyl−N_2.[15] These studies focused on the structures, on the vdW modes, and on the barriers to internal rotation of N_2 in different symmetry environments. N_2 forms a "σ" in-plane complex with phenol,[11] but "π" out-of-plane complexes with the remaining molecules. Evidence for a nearly free internal rotation of the attached N_2 has been provided in most cases.

Here, we present a study of the fully resolved S_1-S_0 electronic spectrum of *p*DFB−N_2 in the collision-free environment of a molecular beam. Two bands are observed in the vicinity of the electronic origin and assigned as the two lowest energy, symmetry-distinguishable transitions involving N_2 internal rotation. Analysis of these two bands provides information about the structures and internal motions of *p*DFB−N_2 in both electronic states. No complex-induced change in the TM orientation is observed. However, there is a significant change in the intermolecular potential energy surface when the photon is absorbed.

Experimental Section

p-Difluorobenzene (*p*DFB) was purchased from Aldrich (99%) and used without further purification. Dry helium (99.9%) and nitrogen (99.9%) gas were used in all experiments. High-resolution data were obtained using the CW molecular beam laser spectrometer described in detail elsewhere.[16] *p*DFB was heated to about 300 K, seeded in a mixture of 10−15% N_2 in He at a backing pressure of about 0.5 bar, expanded through a 280 μm quartz nozzle, skimmed once, and probed 15 cm downstream of the nozzle by a frequency doubled, single-frequency, tunable ring dye laser operating with rhodamine 110, yielding about 200 μW of ultraviolet radiation. Fluorescence was collected using spatially selective optics, detected by a photomultiplier tube and photon counting system, and processed by a computerized data acquisition system. Relative frequency calibrations of the spectra were performed using a near-confocal interferometer having a mode-matched FSR of 299.7520 ± 0.0005 MHz at the fundamental frequency of the dye laser. Absolute frequencies in the spectra were determined by

† Part of the special issue "Charles S. Parmenter Festschrift".

10.1021/jp035201e CCC: $25.00 © 2003 American Chemical Society
Published on Web 10/18/2003

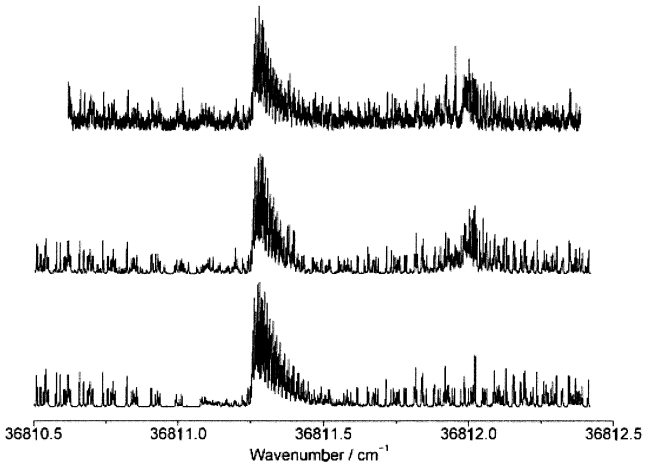

Figure 1. Rotationally resolved fluorescence excitation spectrum of the 0_0^0 band in the $S_1 \leftarrow S_0$ transition of *p*-difluorobenzene−dinitrogen (*p*DFB−N_2). Below the experimental spectrum (top), the simulated spectrum of the stronger subband (bottom) and a simulation using the semirigid internal rotation model (middle trace) are shown.

comparison to transition frequencies in the electronic absorption spectrum of I_2.[17]

Results

Figure 1 shows the rotationally resolved $S_1 \leftarrow S_0$ fluorescence excitation spectrum of the N_2 van der Waals complex of *p*DFB. This spectrum differs from that of the bare molecule in three ways. First, the origin band is shifted by -26.6 cm^{-1} with respect to that of the bare molecule. Second, the band types of the two spectra differ. Whereas the bare molecule exhibits a pure *b*-type spectrum, showing no central Q branch,[18] the spectrum of *p*DFB−N_2 exhibits an obvious Q branch and follows *c*-type selection rules. Third, the origin band of the complex is split into two torsional subbands, separated by 0.71 cm^{-1}, with significantly different relative intensities, approximately 2:1. The electronic origin of the bare molecule consists of only a single strong band.

Fits of the stronger subband spectrum in Figure 1 were initiated by constructing the rotational energy level diagrams of *p*DFB−N_2 in its S_0 and S_1 electronic states, applying the appropriate selection rules, and calculating the frequencies of the allowed rovibronic transitions, for comparison with experiment. The calculated rotational constants were obtained from an optimized geometric structure, based in part on ab initio calculations. Both states were initially assumed to be rigid, asymmetric tops. The simulated spectrum was then compared with the experimental spectrum and several transitions were assigned. These assignments were iteratively optimized by a least-squares analysis. This analysis, though satisfactory in some respects, gave a standard deviation of the fit that was unusually high (observed minus calculated (OMC) = 9.0 MHz). An inspection of this fit revealed that high J ($J \geq 10$) transitions were shifted by as much as 100 MHz with respect to their calculated positions. Therefore, Watson's quartic distortion terms[19] were added to the Hamiltonians of both electronic states. This modification led to an improved OMC of 4.4 MHz, when 200 lines were included in the fit. Unfortunately, the weaker subband in Figure 1 could not be fit by either of these procedures, as shown in Figure 2.

From the stronger subband fit, we determined the origin band frequency and the inertial constants of the two electronic states. These are listed in Table 1. The relative intensities of the transitions could be fit to a rotational temperature of about 5 K. The Lorentzian line width is about 15 MHz in the bare molecule and about 40 MHz in the complex. Thus, the weakly bound N_2 molecule reduces the fluorescence lifetime of *p*DFB from about 11 to 4 ns. Incipient VP and/or IVR may be responsible for this behavior.[20]

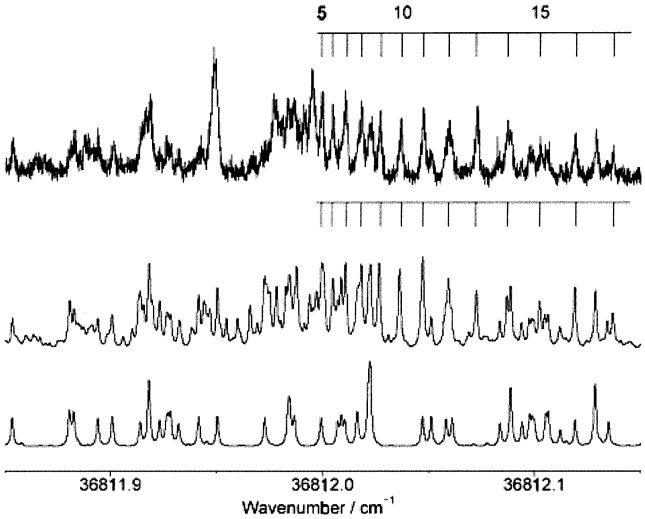

Figure 2. Portion of the fluorescence excitation spectrum of *p*DFB−N_2 near the origin of the weaker subband. Below the experimental spectrum (top), the simulated spectrum of the stronger subband (bottom) and a simulation using the semirigid internal rotation model (middle trace) are shown. Only the Q branch with $K_c' = K_c'' = J$ marked in the spectrum is well reproduced by the calculation.

TABLE 1: Rotational Constants of *p*-Difluorobenzene and *p*-Difluorobenzene−Dinitrogen in Their S_0 and S_1 Electronic States[a]

	ground state		excited state	
parameter	monomer[b]	N_2 complex	monomer	N_2 complex
A/MHz	5637.6(2)	1364.8(4)	5283.2(2)	1391.8(3)
B/MHz	1428.0(1)	1128.3(4)	1434.2(1)	1126.1(3)
C/MHz	1139.4(1)	803.9(25)	1128.5(1)	818.1(25)
Δ_K/MHz		0.034(48)		0.026(47)
Δ_{JK}/MHz		−0.062(71)		−0.052(70)
Δ_J/MHz		0.029(22)		0.029(22)
δ_K/MHz		0.056(35)		0.064(37)
δ_J/MHz		−0.019(11)		−0.019(12)
κ	−0.872	0.153	−0.853	0.072
N[c]	350	167		
OMC/MHz[d]	3.0	4.4		
υ_0/cm^{-1} [e]	36837.84	36811.25		

[a] Uncertainties of the last digits are given in parentheses. [b] Our values, which compare favorably to literature values (ref 18). [c] Number of single transitions included in the fit. [d] Standard deviation of the fit. [e] Origin frequencies. Precision 0.01 cm^{-1}.

Geometry of the Complex. Information about the geometry of the complex can be obtained from its planar moments of inertia (P). These are related to the ordinary moments of inertia (I) by $P_a = (I_b + I_c - I_a)/2$, etc. Values of these for both *p*DFB and *p*DFB−N_2 are listed in Table 2.

In the bare molecule, the *c* inertial axis is perpendicular to the ring plane and the *a* inertial axis lies in the plane, passing through the fluorine atoms. Examining the data in Table 2, we see that P_a (*p*DFB−N_2) ($=P_a$) $\approx$ P_a (*p*DFB) ($=P_a^m$). This means that the orientation of the *a* axis in *p*DFB is unchanged on complexation. We also see that $P_c \approx P_b^m$. This means that the orientations of the *b* and *c* axes are exchanged when the N_2 is attached, thus explaining why the 0_0^0 band of *p*DFB−N_2 is *c* axis polarized. The S_1-S_0 transition moment of the complex still lies in the plane of *p*DFB, roughly perpendicular to *a*.

TABLE 2: Moments of Inertia I and Planar Moments of Inertia P of *p*-Difluorobenzene (*p*DFB) and Its Nitrogen Complex, and Differences between the Moments of Inertia of the Complex and the Monomer[a]

		*p*DFB		*p*DFB−N_2	
	parameter	I^m	P^m	I	P
S_0	a	89.64(1)	353.91(2)	370.3(1)	353.1(10)
	b	353.91(2)	89.64(2)	447.9(2)	275.5(10)
	c	443.55(4)	0.00(2)	628.7(20)	94.8(10)
	$a - a^m$			280.8(1)	−0.8(7)
	$b - c^m$			4.5(2)	275.5(11)
	$c - b^m$			274.7(20)	5.1(10)
S_1	a	95.66(1)	352.28(2)	363.1(1)	351.7(10)
	b	352.38(2)	95.56(2)	448.8(1)	266.0(10)
	c	447.83(4)	0.10(2)	617.8(19)	97.1(10)
	$a - a^m$			267.5(1)	−0.6(10)
	$b - c^m$			1.0(1)	265.9(11)
	$c - b^m$			265.4(19)	1.5(10)

[a] All values in amu Å^2. Uncertainties in the last digits are given in parentheses.

Table 2 also lists values of the differences in the relevant planar moments of *p*DFB−N_2, from which more structural information can be obtained. Thus, among the differences $P_a - P_a^m$, $P_b - P_c^m$, and $P_c - P_b^m$, $P_b - P_c^m$ is by far the largest. A large $P_b - P_c^m (P_c^m \approx 0)$ requires that the N_2 molecule lies on top (or the bottom) of the benzene ring (in both electronic states). A complex configuration with the N_2 molecule lying in or near the plane of *p*DFB would require $P_b \approx 0$ and *a*- and/or *b*-type selection rules.

Of further interest are the values of $P_a - P_a^m$ and $P_c - P_b^m$. Though small, neither of these planar moment differences is zero. This means that the N_2 molecule cannot be attached to *p*DFB "end-on", perpendicular to the complex *ac* plane. Instead, the N_2 molecule must lie more or less in a plane parallel to the *ac* plane. The value of the moment of inertia of the N_2 molecule is 8.5 amu Å^2.[21] Neither planar moment difference in *p*DFB−N_2 is as large as this, but $P_c - P_b^m = 5.1$ amu Å^2 and $P_a - P_a^m = -0.8$ amu Å^2 in the S_0 state. This suggests that the N≡N axis is roughly parallel to the complex *c* axis in this state. $P_c - P_b^m$ is significantly smaller in the S_1 state, being approximately equal (in magnitude) to $P_a - P_a^m$. This suggests that the preferred orientation of the N≡N axis changes when the photon is absorbed.

A more rigorous treatment of this problem requires that the effects of large amplitude motion be taken into account. Two types of motion would seem to be important, "radial" motions and "angular" ones. Radial motions result in displacements of the N_2 molecule's center of mass (COM) from its equilibrium position. Angular motions result in tilts of the N_2 molecule's N≡N bond axis with respect to its equilibrium position. Both types of motion should be fast on the time scale of overall molecular rotation. Thus, the measured rotational constants are vibrationally averaged values over both kinds of coordinates.

Previous studies of the dynamical properties of similar complexes in the gas phase[22] suggest that the intermolecular potential energy surface is relatively steep along the radial coordinate, and relatively flat along the angular ones. The same would be expected to be true for *p*DFB−N_2.[6] Therefore, radial motions are ignored in what follows. Angular motions are taken into account by defining the coordinates ρ and τ shown in Figure 3. ρ is the "tilt" angle between the N≡N axis and the axis perpendicular to the plane (the *c* axis of *p*DFB, $\rho = 90°$ in the parallel configuration), and τ is the "torsional" angle that describes the orientation of the N≡N axis projected onto the *ab* plane of *p*DFB ($\tau = 0°$ when the N≡N axis is parallel to the *a* axis). Using these coordinates, a set of equations can be written that describe the relations between the moments and products of inertia of the complex $I_{\alpha\alpha'}$ ($\alpha, \alpha' = a, b, c$) and those of the bare molecule I_α^m. These are[23]

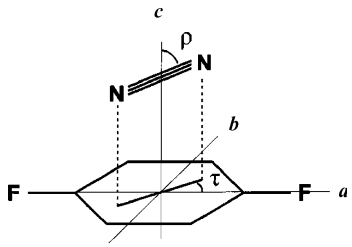

Figure 3. Geometry of the *p*DFB−N_2 complex. The position of the center of mass of N_2 is defined in the principal axis system (*a*, *b*, *c*) of the bare molecule; the orientation of N_2 is defined by ρ (angle between the molecular axis of N_2 and the *c* axis) and τ (angle of rotation of N_2 around the *c* axis). The figure assumes that this axis is perpendicular to the plane.

$$I_a = I_a^m + (\sin^2\tau \sin^2\rho + \cos^2\rho) I_{N_2} + \mu(b^2 + c^2) \quad (1)$$

$$I_b = I_c^m + \sin^2\rho I_{N_2} + \mu(a^2 + b^2) \quad (2)$$

$$I_c = I_b^m + (\cos^2\tau \sin^2\rho + \cos^2\rho) I_{N_2} + \mu(a^2 + c^2) \quad (3)$$

$$I_{ab} = -\cos\tau \sin\rho \cos\rho I_{N_2} - \mu ac \quad (4)$$

$$I_{ac} = -\sin\tau \cos\tau \sin^2\rho I_{N_2} - \mu ab \quad (5)$$

$$I_{bc} = -\sin\tau \sin\rho \cos\rho I_{N_2} - \mu bc \quad (6)$$

Here, $\mu = m_{N_2} m_{DFB}/(m_{N_2} + m_{DFB}) = 22.4839$ amu is the reduced mass of the complex, and *a*, *b*, and *c* are the COM coordinates of the attached N_2 molecule in the principal axis system of the bare molecule (cf. Figure 3). The potential $V(\tau)$ should be 2-fold symmetric, given the likely electronic distribution of *p*DFB in both states. (Only a motion that interchanges the nitrogen nuclei can explain the observed 2:1 intensity ratio between the two subbands in the UV spectrum.) Hence, averaging over τ should result in zero values for $\langle a \rangle$ and $\langle b \rangle$; the COM of the attached N_2 should lie on *c*. (More rigorously, $\langle a \rangle$ and $\langle b \rangle$ should be zero due to averaging over the zero-point motion of the N_2 COM in the G_{16} molecular symmetry group of the complex.) Similarly, the average values of $\langle \sin\tau \rangle$ and $\langle \cos\tau \rangle$ also should be zero. Thus, because I_{ab}, I_{ac}, and I_{bc} (eqs 4−6) are zero, I is diagonal.

We now use eqs 1−3 to obtain estimates of $\langle a^2 \rangle$, $\langle b^2 \rangle$, $\langle c^2 \rangle$, ρ, and τ in both electronic states. Unfortunately, there is not enough information to determine all of these parameters independently. So, we first treat the attached N_2 as a point particle with mass μ and ignore its moment of inertia I_{N_2}. Equations 1−3 then reduce to the familiar equations of Kraitchman.[23] Comparisons of the experimental moments I_a, etc. of the complex with the corresponding moments I_a^m, etc. of the bare molecule then yield estimates of the mean square displacements $\langle a^2 \rangle$, $\langle b^2 \rangle$, and $\langle c^2 \rangle$ of the COM of the attached N_2 in both electronic states. These are listed in Table 3. Examining these data, we see that $\langle c^2 \rangle^{1/2} = 3.53$ Å in the S_0 state and $\langle c^2 \rangle^{1/2} = 3.45$ Å in the S_1 state. The decrease in $\langle c^2 \rangle^{1/2}$ in the S_1 state is consistent with the red shift of the $S_1 - S_0$ origin band of *p*DFB−N_2 relative to the bare molecule; N_2 is more

TABLE 3: Mean Square Displacements of the Nitrogen Molecule in the Principal Axis System of *p*DFB, in Its S_0 and S_1 Electronic States[a]

parameter	ground (S_0) state	excited (S_1) state
$\langle a^2\rangle^{1/2}$/Å	0.09(2)	0.08(2)
$\langle b^2\rangle^{1/2}$/Å	0.69(2)	0.35(2)
$\langle c^2\rangle^{1/2}$/Å	3.53(1)	3.45(1)
R_{eff}/Å	3.49(1)	3.42(1)

[a] Uncertainties in parentheses.

strongly bound in the S_1 state. The values of $\langle a^2\rangle^{1/2}$ are relatively small and the values of $\langle b^2\rangle^{1/2}$ are relatively large, in both electronic states. Previous studies of rare gas complexes of aromatic molecules have yielded vibrationally averaged in-plane coordinates that are more nearly equal, as in 1-fluoronaphthalene−Ar and 2-fluoronaphthalene−Ar.[21] In contrast, *p*DFB−N_2 exhibits very different values of the two, $\langle a^2\rangle^{1/2} = 0.09$ Å and $\langle b^2\rangle^{1/2} = 0.69$ Å in the S_0 state. These data suggest that the N_2 molecule moves with significantly larger amplitude (or has significantly greater spatial extent) along *b* than along *a*, which again supports the idea that it is preferentially oriented along *b*, rather than *a*. The value of $\langle b^2\rangle^{1/2}$ is much smaller in the S_1 state. All of these values are subject to some uncertainty, given the poorly defined potentials along the intermolecular coordinates. But they have at least some quantitative significance.

Next, we re-express eqs 1−3 in terms of the planar moment differences $P_a - P_a^m$, $P_b - P_c^m$, and $P_c - P_b^m$, obtaining

$$P_a - P_a^m = \frac{1}{2}(1 + \langle\cos 2\tau\rangle)\sin^2 \rho I_{N_2} + \mu\langle a^2\rangle \qquad (7)$$

$$P_b - P_c^m = \cos^2 \rho I_{N_2} + \mu\langle c^2\rangle \qquad (8)$$

$$P_c - P_b^m = \frac{1}{2}(1 - \langle\cos 2\tau\rangle)\sin \rho I_{N_2} + \mu\langle b^2\rangle \qquad (9)$$

Finally, we compare the experimental values of $P_a - P_a^m$, $\langle a^2\rangle$, etc. (Tables 2 and 3) with eqs 7−9, thereby obtaining estimates of $\langle\rho\rangle$ and $\langle\tau\rangle$. Equation 8 yields $\langle\rho\rangle = 45 \pm 10°$ in the S_0 state and $\langle\rho\rangle = 65 \pm 15°$ in the S_1 state. Apparently, the N_2 molecule spends a significant amount of time in near-perpendicular orientations, especially in the ground state. Equations 7 and 9 yield $\langle\tau\rangle = 70 \pm 10°$ in the S_0 state. The corresponding value in the S_1 state is not well determined. Equation 7 gives a similar value, but eq 9 gives a value much lower than this, $\langle\tau\rangle = 15 \pm 10°$. We conclude, then, that the N_2 molecule lies mainly in the plane, parallel to the *b* axis in the S_0 state, but rotates more freely in the S_1 state.

The above analysis is deficient in two respects. First, it neglects possible contributions to *B* from the torsional motion itself. Second, it neglects possible contributions to $\langle a^2\rangle$, $\langle b^2\rangle$, and $\langle c^2\rangle$ from the moment of inertia of the attached N_2. A more rigorous treatment of the latter problem using the relation

$$R_{eff}^2 = \frac{1}{2\mu}[I_a + I_b + I_c - (I_a^m + I_b^m + I_c^m) - 2I_{N_2}] \qquad (10)$$

yields the COM distances from the N_2 to the ring of $R_{eff}(S_0) = 3.474(7)$ Å and $R_{eff}(S_1) = 3.390(6)$ Å, values that are independent of the value of ρ. If the effects of internal rotation are also taken into account, then assuming $\rho = 90°$ leads to $R_{eff} = 3.487(12)$ Å and $\tau = 68(14)°$ in the S_0 state, and $R_{eff} = 3.415(11)$ Å and $\tau = 52(10)°$ in the S_1 state.

Mean torsional amplitudes $\overline{\Delta\tau} = (\Delta\tau^2)^{1/2}$ can be obtained by expanding $\langle\cos 2\tau\rangle = \langle\cos 2(\tau_e + \Delta\tau)\rangle$ as a Taylor series, which yields for $\tau_e = 0$ or 90°

$$\langle\cos 2\tau\rangle_{\tau_e} = 0 = -\langle\cos 2\tau\rangle_{\tau_e} = 90 = \langle\cos 2\Delta\tau\rangle \approx \cos 2\overline{\Delta\tau} \qquad (11)$$

where $\langle\Delta\tau^{2n}\rangle \approx \langle\Delta\tau^2\rangle^n$ has been used in the approximation of eq 11. With this approximation, 22° and 38° were obtained for $\overline{\Delta\tau}$ in S_0 and S_1, respectively. Such large amplitudes clearly indicate that the barriers hindering internal motion are quite low in both electronic states.

Barriers to Internal Rotation. Estimates of the barriers to internal motion in *p*DFB−N_2 may be obtained in the following way. First, we assume that the N_2 molecule is rigidly attached to *p*DFB with its N≡N axis lying in a plane parallel to the *ab* plane. We further assume the N_2 exhibits a hindered rotation about the *c* axis, which is governed by a 2-fold potential, $V_2(\tau)$. In that event, $\rho = 90°$, $\langle a^2\rangle = \langle b^2\rangle = 0$, and $B_{rigid} = \{\hbar^2\}/\{(2h[I_c^m + I_{N_2}])\}$, from eq 2. The difference between this "rigid-body" value of *B* and the observed B_{eff} can then be used to estimate V_2 via the relation[24]

$$B_{eff} - B_{rigid} = FW_A^2\left(\frac{I_{N_2}}{I_c^m + I_{N_2}}\right)^2 \qquad (12)$$

where *F* is the internal rotor constant

$$F = \frac{\hbar^2}{2hI_{N_2}}\left(\frac{I_c^m + I_{N_2}}{I_c^m}\right) = 60.78 \text{ GHz} \qquad (13)$$

and W_A^2 is a second-order perturbation coefficient. In the high barrier approximation, this coefficient can be related to the energy difference between the two lowest torsional states, ΔE[24]

$$W_A^2 = -\frac{1}{2}\pi^2 w_1 \approx \frac{1}{4}\pi^2(b_2 - b_1) = \frac{1}{4}\pi^2\frac{\Delta E}{F} \qquad (14)$$

from which the reduced barrier height,

$$s = 4V_N/(N^2F) \qquad (15)$$

can be derived. This simple model yields $s = 6.16$ and $V_2 = 12.5$ cm^{-1} for the S_0 state and $s = 3.85$ and $V_2 = 7.8$ cm^{-1} for the S_1 state.

The difference between the calculated torsional splittings in the two states ($\Delta E = 11.9$ GHz in S_0 and $\Delta E = 21.8$ GHz in S_1) is too small to explain the observed separation of the two subbands in the spectrum, 21.3 GHz. Thus, the actual barriers are likely to be smaller than the above estimates. (In agreement with this, the simple model (eq 12) gives only an upper limit to V_2.) V_2 barriers of about 10 and 2.5 cm^{-1} in the two states yield values of $\langle\cos 2\tau\rangle$ that are similar to the observed ones, on the basis of simulations using an effective Hamiltonian for the large amplitude motion.[25] With such small barriers, the high barrier approximation may be unreliable.

More rigorously, the spectrum was analyzed with the aid of the semirigid internal rotor model described elsewhere.[26] Torsional levels ($J = 0$) were calculated for different potentials $V_2(\tau)$. Taking the distance between the two *Q* branches in the spectrum (21.3 GHz) as the difference $\Delta E' - \Delta E''$, it was evident that $|V_2'| < |V_2''|$ and that $|V_2'| < 7.5$ cm^{-1}. A comparison of these results with the frequencies of the torsional

sidebands observed in the REMPI spectrum of *p*DFB−N_2[9] suggests $V_2' \approx 2$ cm^{-1}.

Next, attempts were made to least-squares fit the rotational structure of both subbands simultaneously, by varying both the moments of inertia of the complex and the potential energy terms, in both states. Initially, rigid rotor Hamiltonians and potentials containing only V_2 terms were employed. Later, centrifugal distortion and structural relaxation terms[23] were included in the rotational Hamiltonians, and V_4 terms were added to the potential. The best fits were obtained when the N_2 molecule was oriented parallel to *c* in the S_0 state, in accord with the previous conclusion. No obvious preference was detected for the S_1 state.

Despite these attempts, it was not possible to fully reproduce the observed spectrum of the weaker subband. Figure 2 shows a typical example. Here, $V_2'' = 7.2$ cm^{-1}, $V_2' = 2.2$ cm^{-1}, and $V_4'' = V_4' = 0$; yielding a predicted subband splitting of 22.4 GHz, in approximate agreement with experiment (21.3 GHz). Including modest centrifugal distortion and structural relaxation terms leads to a fit of 224 single transitions with an OMC of 7.3 MHz. Still, principally due to spectral overlap, only the Q branch with $K_c' = K_c'' = J$ and some P branch transitions could be fit, as shown in Figure 2. A possible explanation for this behavior is that the second lowest torsional level in S_1, in which the weaker subband likely terminates, is just above the barrier and is likely perturbed by torsion−rotation interactions. Further, the amplitude of internal rotation should increase dramatically above the barrier, influencing significantly the measured moments of inertia.[27] A similar problem exists for benzene−N_2, which also has very small torsional barriers. Only the high resolution spectra of the lowest $m = 0$ torsional levels have been successfully analyzed to date.[3,4]

Our conclusions regarding the equilibrium geometry and magnitude of the barrier to internal rotation of *p*DFB−N_2 in its ground electronic state are consistent with the recent ab initio calculations of Chen and Davidson.[28] These authors found that the BSSE-corrected geometry of *p*DFB−N_2 is the "perpendicular" one ($\tau = 90°$), irrespective of method (MP2, MP3, and MP4 (SDQ)) and (high-level) basis set and that the barrier is "only a few cm^{-1}".

Most models developed by us to interpret the high-resolution spectra of *p*DFB−N_2 reproduce well the splittings observed in the low resolution spectrum of the Parmenter group.[1] These splittings are thus attributed to the contributions of torsional sidebands to the spectrum, rather than hybrid band character. Both of the bands studied in this work are pure *c*-type bands. It is possible that the 6_0^1 band is different, but we consider this unlikely.

Discussion

Apart from this negative result, that there is no *complex*-induced electronic TM rotation in *p*DFB−N_2, the most interesting finding in this work is that there is a substantial change in the barrier to internal rotation of the attached N_2 when the complex absorbs light, from $V_2 \sim 10$ cm^{-1} in the S_0 state to $V_2 \sim 2$ cm^{-1} in the S_1 state. The N≡N bond axis is more or less uniquely oriented along the short in-plane axis in the ground S_0 state but essentially free to assume any orientation parallel to the aromatic plane in the excited S_1 state. This result is, at first glance, even more surprising when one realizes that the binding energy of the complex must *increase* on electronic excitation, because the S_1−S_0 origin of *p*DFB−N_2 is shifted to the red of the corresponding origin of the bare molecule by ~27 cm^{-1}. A stronger vdW bond is also indicated by the observed decrease in R_{eff} (Table 3) on S_1 excitation.

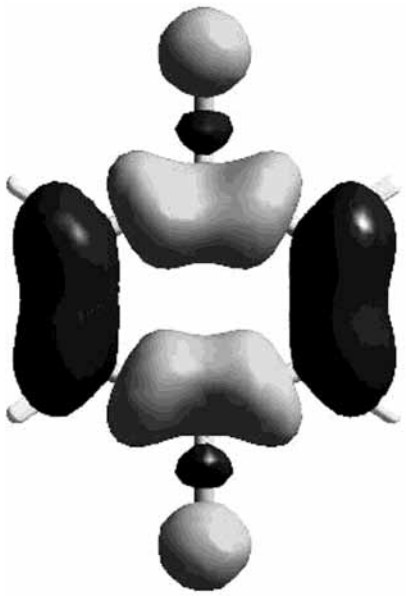

Figure 4. Electron density difference map for the $S_1 \leftarrow S_0$ transition of *p*DFB. Black contours indicate regions of electron gain, and gray contours indicate regions of electron loss.

This apparent dilemma is resolved when one realizes that V_2 barriers are measures of the *anisotropy* of the potential in the aromatic plane, not of its average values. Large differences in either the attractive or the repulsive terms in orientations parallel to *a* and parallel to *b* will give rise to large barriers. Conversely, if there are only small differences in these terms, and V_2 is more isotropic, the internal rotation will be nearly free. Seemingly, this is the case in the S_1 state of *p*DFB−N_2.

Probing this issue further, we have performed ab initio calculations on *p*DFB in its S_0 and S_1 electronic states using the Gaussian 98 suite of programs.[29] A 6-31G** basis set was employed; the MP2 method was used for the S_0 state, and the CIS method was used for the S_1 state. These calculations qualitatively reproduce the changes in the rotational constants that occur when the molecule absorbs light; i.e., a large decrease in *A*, and smaller changes in *B* and *C* (cf. Table 1). As is well-known, these changes are a consequence of a quinoidal distortion of the ring. The S_1 state has significantly shorter parallel ring C−C bonds than "perpendicular" ones.

If there are significant differences in the geometries of the two states of *p*DFB, then there must also be significant differences in their electron distributions. Figure 4 shows an electron density difference map for *p*DFB, illustrating clearly that the absorption of light produces a large change in the distribution of π electrons around the ring. In particular, π-electron density shifts from regions parallel to the C−F bonds (along the long axis) to regions perpendicular to these bonds (along the short axis). It is thus reasonable to suggest that these changes in electron distribution are primarily responsible for the significant differences in the barrier heights in S_0 and S_1 *p*DFB−N_2.

*p*DFB and N_2 are both quadrupolar molecules; owing to their high symmetry, their first nonvanishing multipole moments are the quadrupole moments, as shown below:

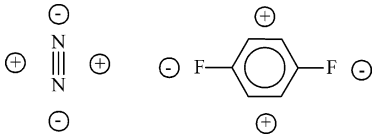

TABLE 4: Quadrupole Moments of *p*-Difluorobenzene in Its S_0 and S_1 Electronic States, According to Theory (MP2/CIS 6-31G)**

parameter[a]	S_0	S_1
Q_a	−19.27	−9.64
Q_b	+19.18	+12.62
Q_c	+0.10	−2.97

[a] In units of Debye Å, in the inertial coordinate system of *p*DFB.

Clearly, the stable configuration of the S_0 state of *p*DFB−N_2 should be one in which the N_2 is attached to the top (or bottom) of the aromatic plane, perpendicular to the two C−F bonds. This is exactly what is observed. But excitation of *p*DFB by light changes its "in-plane" electron distribution and could therefore change both the preferred orientation of the N≡N bond axis and the barrier opposing its motion.

Table 4 lists the quadrupole moments of *p*DFB in its S_0 and S_1 electronic states, according to theory. As expected, the quadrupole tensor of S_0 *p*DFB is nearly axially symmetric about *c*; it is large and negative along *a*, and equally large and positive along *b*. The predicted anisotropy is ∼38 D Å. The corresponding tensor of S_1 *p*DFB is significantly different; it is both less symmetric, and less anisotropic. $Q_b - Q_a$ is ∼22 D Å, a 40% reduction compared to the ground state. The larger value of Q_c no doubt is partially responsible for increasing the binding energy of the attached N_2. More importantly, the decrease in $Q_b - Q_a$ clearly indicates that the "in-plane" π-electron distribution is more isotropic in the S_1 state and thus explains the large decrease in V_2 in this state.

This situation stands in sharp contrast to that in aniline−N_2.[13] Here, a large increase in barrier height is observed on S_1-S_0 excitation, from ∼25 cm^{-1} in the S_0 state to ∼65 cm^{-1} in the S_1 state. But N_2 is bound by a dipole−induced dipole interaction in aniline−N_2, leading to an equilibrium geometry (in both states) in which the N≡N bond axis is parallel to the *long* axis of the ring. And excitation of aniline to its S_1 state leads to a large increase in its dipole moment along this axis,[30] thus explaining the large increase in V_2 in this system.

Clearly, future studies of this type will provide valuable data that may be used to benchmark intermolecular potentials, so important in both *intra* and *inter*molecular dynamics.

Acknowledgment. This work is dedicated to celebrating the career of Professor C. S. Parmenter at Indiana University on the occasion of his 70th birthday. It was supported in part by NSF (CHE-9987048). M.S. thanks the Schweizerischer Nationalfonds for a postdoctoral fellowship.

References and Notes

(1) Ju, Q.; Parmenter, C. S. Abstract MH07, 53rd International Symposium on Molecular Spectroscopy, Columbus, OH, 1998. See also: Ju, Q. Ph.D. Thesis, Indiana University, December, 1998.

(2) Joireman, P. W.; Kroemer, R. T.; Pratt, D. W.; Simons, J. P. *J. Chem. Phys.* **1996**, *105*, 6075.

(3) Weber, Th.; Smith, A. M.; Riedle, E.; Neusser, H. J.; Schlag, E. W. *Chem. Phys. Lett.* **1990**, *175*, 79.

(4) Ohshima, Y.; Kohguchi, H.; Endo, Y. *Chem. Phys. Lett.* **1991**, *184*, 21.

(5) Neusser, H. J.; Sussman, R.; Smith, A. M.; Riedle, E.; Weber, Th. *Ber. Bunsen-Ges. Phys. Chem.* **1992**, *96*, 1252.

(6) Lee, S.; Romascan, J.; Felker, P. M.; Pedersen, T. B.; Fernández, B.; Koch, H. *J. Chem. Phys.* **2003**, *118*, 1230.

(7) Gilbert, B. D.; Parmenter, C. S.; Su, M.-C.; Oh, H.-K.; Zhao, Z.-Q. *Appl. Phys.* **1994**, *B59*, 397.

(8) Gilbert, B. D.; Parmenter, C. S.; Oh, H.-K. *J. Phys. Chem.* **1995**, *99*, 2444.

(9) Hu, Y.; Lu, W.; Yang, S. *J. Photochem. Photobiol.* **1997**, *A106*, 91.

(10) Hu, Y.; Lu, W.; Yang, S. *J. Chem. Phys.* **1996**, *105*, 5305.

(11) Ford, M. S.; Haines, S. R.; Pugliesi, I.; Dessent, C. E. H.; Müller-Dethlefs, K. *J. Electron Spectrosc.* **2000**, *112*, 231.

(12) Yamanouchi, K.; Isogai, S.; Tsuchiya, S. *J. Mol. Struct.* **1986**, *146*, 349.

(13) Schäfer, M.; Pratt, D. W. *J. Chem. Phys.* **2001**, *115*, 11147.

(14) Disselkamp, R.; Bernstein, E. R. *J. Chem. Phys.* **1993**, *98*, 4339.

(15) Sun, S.; Bernstein, E. R. *J. Chem. Phys.* **1995**, *103*, 4447.

(16) Majewski, W. A.; Pfanstiel, J. F.; Plusquellic, D. F.; Pratt, D. W. In *Laser Techniques in Chemistry*; Myers, A. B., Rizzo, T. R., Eds.; Wiley: New York, 1995; pp 101−148.

(17) Gerstenkorn, S.; Luc, P. *Atlas du spectre d'absorption de la molécule d'iode* CNRS: Paris, 1978.

(18) Sussman, R.; Neuhauser, R.; Neusser, H. J. *Can. J. Phys.* **1994**, *72*, 1179.

(19) Watson, J. K. G. In *Vibrational Spectra and Structure*; Durig, J. R., Ed.; Elsevier: Amsterdam, 1977; Vol. 6, p 1 (see also references therein).

(20) Sinclair, W. E.; Pratt, D. W. *J. Chem. Phys.* **1996**, *105*, 7942.

(21) Lofthus, A.; Krupenie, P. H. *J. Phys. Chem. Ref. Data* **1977**, *6*, 113.

(22) See, for example: Champagne, B. B.; Pfanstiel, J. F.; Pratt, D. W.; Ulsh, R. C. *J. Chem. Phys.* **1995**, *102*, 6432.

(23) Gordy, W.; Cook, R. L. *Microwave Molecular Spectra*, 3rd ed.; Wiley-Interscience: New York, 1984.

(24) Herschbach, D. R. *J. Chem. Phys.* **1959**, *31*, 91.

(25) Makarewicz, J. *J. Mol. Spectrosc.* **1996**, *176*, 169.

(26) Schäfer, M. *J. Chem. Phys.* **2001**, *115*, 11139.

(27) Borst, D. R.; Pratt, D. W. *J. Chem. Phys.* **2000**, *113*, 3658.

(28) Chen, F.; Davidson, E. R. *Chem. Phys. Lett.* **2002**, *360*, 99.

(29) Frisch, M. J.; Trucks, G. W.; Schlegel, H. B.; Scuseria, G. E.; Robb, M. A.; Cheeseman, J. R.; Zakrzewski, V. G.; Montgomery, J. A.; Stratmann, R. E.; Burant, J. C.; Dapprich, S.; Millam, J. M.; Daniels, A. D.; Kudin, K. N.; Strain, M. C.; Farkas, O.; Tomasi, J.; Barone, V.; Cossi, M.; Cammi, R.; Mennucci, B.; Pomelli, C.; Adamo, C.; Clifford, S.; Ochterski, J.; Petersson, G. A.; Ayala, P. Y.; Cui, Q.; Morokuma, K.; Malick, D. K.; Rabuck, A. D.; Raghavachari, K.; Foresman, J. B.; Cioslowski, J.; Ortiz, J. V.; Baboul, A. G.; Stefanov, B. B.; Liu, G.; Liashenko, A.; Piskorz, P.; Komaromi, I.; Gomperts, R.; Martin, R. L.; Fox, D. J.; Keith, T.; Al-Laham, M. A.; Peng, C. Y.; Nanayakkara, A.; Challacombe, M.; Gill, P. M. W.; Johnson, B. G.; Chen, W.; Wong, M. W.; Andres, J. L.; Gonzalez, C.; Head-Gordon, M.; Replogle, E. S.; Pople, J. A. *Gaussian 98*, Revision A.9; Gaussian, Inc.: Pittsburgh, PA, 1998.

(30) Korter, T. M.; Borst, D. R.; Butler, C. J.; Pratt, D. W. *J. Am. Chem. Soc.* **2001**, *123*, 96.